Malaysian Journal of Mathematical Sciences 5(1): 61-83 (2011)

A Study of the Pseudostate-Close-Coupling Method Using a Non-Orthogonal Laguerre-L^2 Basis in the Intermediate Energy

[1]Agus Kartono and [2]Mustafa Mamat
[1]Laboratory for Theoretical and Computational Physics, Department of Physics, Faculty of Mathematical and Natural Sciences, Institut Pertanian Bogor, Kampus IPB Darmaga, Bogor 16680, Indonesia
[2]Department of Mathematics, Faculty of Sciences and Technology, Universiti Malaysia Terengganu, 21030 Kuala Terengganu, Terengganu, Malaysia
E-mail: [1]akartono@ipb.ac.id and [2]mus@umt.edu.my

ABSTRACT

We present the pseudostate-close-coupling method using a non-orthogonal Laguerre-L^2 basis function for the calculations of electron-helium scattering. Our method is a frozen-core model of the target in which one of the electrons is restricted to the 1*s* He^+ orbital. The non-orthogonal Laguerre-L^2 basis function has been applied in the intermediate energy region (30, 40 and 50 eV) for the electron impact elastic and excitation of the 2^1S, 2^1P, 2^3S and 2^3P states of helium. Differential and integrated cross sections are calculated and compared with recent experiments. The present calculation (PC) results for each case are discussed and compared with other calculations. It is found that the results agree quite well with experiments and with the other calculations.

Keywords: Non-orthogonal Laguerre-L^2 basis, Elastic and excitation, Intermediate energy, frozen-core model, Differential and integrated cross sections

INTRODUCTION

Collision processes involving helium are important in plasmas, lasers, planetary atmospheres, interstellar space, and many other environments. The measurement of cross sections for collisions with helium has been ongoing for over 40 years. Helium is an ideal choice because of the central role of being the simplest many electron atom for many different theoretical and experimental studies and the fact that it is widely used to normalize and calibrate results obtained from more complex targets.

The ab initio calculation of cross sections is challenging for two reasons. First, very accurate ground and excited state wave functions are required. Second, the fundamental interactions between an electron and a complex atom must be known. At short range, the incident electron becomes part of a transient electron plus target system, so that a detailed treatment of

electronic interactions must be used. At long range, the dominant interaction is Coulomb attraction between the electron and the excess ionic charge. This attractive field for ions means that many partial waves contribute to excitation and that the cross section is finite and non-zero at the threshold energy.

The energy range of interest in atomic physics has been divided into the low (below ionization threshold), intermediate (between one and ten times the ionization threshold) and high (more than ten times the ionization threshold) regions. The ionization threshold of the helium atom is 24.58 eV. Here we primarily concentrate on three energies 30, 40 and 50 eV in the intermediate region. This is in the most difficult intermediate energy range, being only 5.42 to 25.42 eV above the ionization threshold. The intermediate energy region extends up to the incident electron energy where velocity of the incident electron is typically about four times the velocity of the active target electrons. This is most difficult region to treat theoretically since an infinite number of target states can be excited and also ionizing collisions are possible. At intermediate energies, there should be an infinite number of bound target states and also continuum states should be included in the expansion. One approach which has had some success is based on the expansion where some of the target states are replaced by suitably chosen pseudostates which are not eigenstates of the target Hamiltonian. Instead each of these pseudostates represent an average in some sense over the complete set of target eigenstates.

In atomic physics, the L^2 method which uses square integrable (L^2) functions, has been the subject of considerable study for the solution of electron-atom scattering problem. One approach to describing electron scattering from atomic targets is to use pseudostate coupled-channel equations. In this model one uses a finite basis of L^2 functions to diagonalize the target Hamiltonian thus giving both negative and positive energy states. The basis is usually chosen so that the lowest-lying channels are described adequately while the other bound states are collectively approximated by the remaining energy eigenvectors. The positive energy eigenstates and associated L^2 eigenvector in some way approximate the target continuum. The target states cannot all be included in any practical implementation of the electron scattering equations. A pragmatic way to approach such a calculation is to include the effects of the target states which are deemed to be most important, for example in the helium target to choose just the $^{1,3}S$ and $^{1,3}P$ levels. Unfortunately it has been observed that such expansions are inadequate at all but the lowest energies.

There is considerable evidence that the coupling to all open channels must be included in some way. Above the ionization threshold, this means that allowance for coupling to continuum channels must be made. An efficient way to include such coupling is by means of taking a subspace of the one-body Hilbert space of the target. A convenient basis for the one-body Hilbert space is that provided by the Laguerre functions.

In this paper, we apply the L^2 expansion methods for the helium atom used recently by Winata and Kartono (2004) and Kartono *et al*. (2005). The non-orthogonal Laguerre-L^2 basis function will be used and the related expansions for discrete and continuum states will be considered. The finite-basis expansions, considered as approximations to the infinite expansion will be studied and their convergence will be shown. The manner in which the L^2 approximated wave functions are related to the true eigenstates is examined through the underlying Gaussian quadrature. The frozen-core approximation will be used.

In order to develop a general reliable method for the calculation of electron-atom scattering phenomena, the close-coupling (CC) formalism has been chosen. Having expanded the total wave function in a set of target states, it attempts to solve the resulting scattering equations without approximation. The pseudostate-close-coupling (PSCC) method therefore provides a systematic approach to increasing the multi-channel expansion by the use of an increasing non-orthogonal Laguerre basis sizes. In the expansions, completeness is approached and that if the convergence to a required accuracy is observed, then any larger expansions are unlikely to significantly alter the result.

The PSCC method utilizes an expansion of the target in a complete set of non-orthogonal Laguerre-L^2 basis function which forms a basis for the underlying Hilbert space. The PSCC method is the calculations for which, in addition to the treatment of true discrete eigenstates, there are also a number of square-integrable states with positive energies included. These are called pseudostates because they are not true eigenstates of the target Hamiltonian, but are usually obtained by diagonalizing the Hamiltonian in a non-orthogonal Laguerre-L^2 basis function.

In terms of testing the basic assumptions of the pseudostate method and understanding its theoretical justification, the work of several groups deserves mention. Early numerical calculations for the electron-atom problem utilizing pseudostates were carried out by many researchers (Bray and Stelbovics (1992), Fursa and Bray (1995), Bartschat *et al*. (1996)

and references therein). They demonstrated that the inclusion of a few pseudostates significantly reduced the cross sections for scattering, bringing them into better overall agreement with experiment.

In this article, electron impact differential and integrated cross sections of helium are calculated within the PSCC method. Our tests of this approximation for intermediate energy elastic scattering require few expansion states. The former has a maximum of 80 channels and couples a total of 25 states consisting of 7 ^1S, 6 ^3S, 6 ^1P and 6 ^3P. For intermediate energy excitation scattering require many expansion states; we make the former has a maximum of 120 channels and couples a total of 37 states consisting of 7 ^1S, 6 ^3S, 6 ^1P, 6 ^3P, 3 ^1D, 3 ^3D, 3 ^1F and 3 ^3F. For larger bases, calculations are close to the limit of our desk-top workstation computational resources. Comparisons with experiment are made at impact energies 30, 40 and 50 eV to examine the range of validity of the PSCC method.

THEORY

In this section we discuss our method (for review see Winata and Kartono (2004)) of calculating the structure of the helium-target ground and excited states. We have written a general configuration interaction program which diagonalizes the helium Hamiltonian in the anti-symmetrized two-electron basis, where the radial part of the single-particle functions ϕ_{nl} are taken to be the non-orthogonal Laguerre-L^2 basis function

$$\phi_{nl}(r) = (\lambda_l r)^{l+1} \exp(-\lambda_l r/2) L_n^{2l+1}(\lambda_l r), \tag{1}$$

and where the $L_n^{2l+1}(\lambda_l r)$ are the associated Laguerre polynomial, λ_l is the interaction parameter and n ranges from 1 to the basis size N. The two-particle space is written in terms of the product of these orbital for coordinates r_1 and r_2. We may rearrange these products into linear combinations which are eigenvalues of the total orbital angular momentum and total spin function.

The helium atom states in configuration interaction form are (the notation α and β are used to denote the first and second electron)

$$\Phi_{n\pi lm s\upsilon}(x_1, x_2) = \sum_{n_\alpha, n_\beta}^{\infty} C_{n\pi}^{(\alpha\beta)} \left| \varphi_\alpha(x_1) \varphi_\beta(x_2) : \pi_n l_n m s_n \upsilon \right\rangle, \tag{2}$$

where the configurations are chosen so that the selection rules are satisfied for the combination $(\alpha\beta)$ and they are correctly anti-symmetrized two-electron states of parity $(-1)^{l_\alpha + l_\beta}$ with total orbital angular momentum eigenvalues l, m and spin eigenvalues s, υ. Here the configuration interaction coefficients $C_n^{(\alpha\beta)}$ satisfy the symmetry property

$$C_n^{(\alpha\beta)} = (-1)^{l_\alpha + l_\beta - l - s} C_n^{(\beta\alpha)}, \tag{3}$$

to ensure anti-symmetry of the two-electron system states.

The target Hamiltonian H_T is

$$H_T = H_1 + H_2 + V_{12}, \tag{4}$$

where

$$H_i = K_i + V_i = -\frac{1}{2}\nabla_i^2 - \frac{Z}{r_i}, \tag{5}$$

for $i = 1, 2$ is the one-electron Hamiltonian of the He^+ ion $(z = 2)$ and

$$V_{12} = \frac{1}{r_{12}}, \tag{6}$$

is the electron-electron potential. Atomic units (a.u.) are assumed throughout.

Whereas the above Hamiltonian formalism (4) is general and includes two-electron excitation, in practice we have found that it is sufficient to make the frozen-core approximation, where one of the electrons is in a fixed orbital while the second electron is described by a set of independent L^2 functions, thus permitting it to span the discrete and continuum excitations, in which all configurations have one of the electrons occupying the lowest orbital.

The resulting target states $\Phi(x_1, x_2)$ where x is used to denote both the spatial and spin coordinates, satisfy

$$\left\langle \Phi_m \left| -\frac{1}{2}\nabla_1^2 - \frac{Z}{r_1} - \varepsilon_{n_\alpha} \right| \Phi_n \right\rangle = 0, \quad m,n = 1,2,...,N \tag{7}$$

in order to get a good description of the He^+ ion state, where ε_{n_α} is the energy associated with the $1s$ state of He^+ ion. The excitation states for $\Phi(x_1, x_2)$ can be obtained by solving the equation

$$\left\langle \Phi_m \left| -\frac{1}{2}\nabla_2^2 - \frac{Z}{r_2} + \frac{1}{r_{12}} - \varepsilon_{n_\beta} \right| \Phi_n \right\rangle = 0, \qquad m,n = 1,2,...,N \tag{8}$$

where ε_{n_β} is the energy associated with the excitation states of the helium atom.

In our work we simplify the problem by using the frozen-core model. In order to get a good description of the ground states we take $\lambda_0 = 4$ for $N_\alpha = 1$. This choice generates the He^+ $1s$ orbital, which allows us to take into account short-range correlations in the ground state, as well as being able to obtain an accurate representation of excited discrete and continuum states. To obtain good nS excited states we take $\lambda_0 = 0.93$ (triplet and singlet) for $N_\beta > 1$.For nP excited states we takes $\lambda_1 = 0.72$ (triplet) and $\lambda_1 = 0.73$ (singlet), and for nD excited states we take $\lambda_2 = 0.62$ (triplet) and $\lambda_2 = 0.63$ (singlet).

The configuration interaction coefficients $C_{Ni}^{(\alpha\beta)}$ are given by Winata and Kartono (2004) and Kartono *et al.* (2005):

$$\left(C_{Ni}^{(\alpha\beta)}\right)^2 = \frac{2^{2l}}{\pi} \frac{\lambda_l}{\left(1 - X_{Ni}^{(\alpha\beta)}\right)} W_{Ni}^{(\alpha\beta)}, \tag{9}$$

where the labels α and β are used to denote the first and second electron and W_{Ni} are the associated quadrature weights of Gaussian quadrature based Pollaczek polynomial which are given by

$$W_{Ni}^{(\alpha\beta)} = \frac{\pi\Gamma(N+2l+1)}{2^{2l}\Gamma(N+1)} \frac{1}{P_{N-1}^{l+1}\left(X_{Ni}^{(\alpha\beta)}\right)\frac{d}{dx}P_N^l\left(X_{Ni}^{(\alpha\beta)}\right)}. \tag{10}$$

Calculated examples of the configuration interaction coefficients and eigenvalues for nS and nP excited states are presented in Table 1 and Table 2. We see that the convergence of the several lowest states is obtained by increasing the basis size.

The time independent Schrödinger equation for electron scattering from atomic helium is

$$(E-H)\left|\Psi(x_0,x_1,x_2)\right\rangle = 0, \tag{11}$$

where the Hamiltonian

$$H = H_T + H_0 + V_{01} + V_{02}, \tag{12}$$

and the subscript 0 is used to denote the projectile space, and the subscripts 1 and 2 being used for target space. The Hamiltonian target operator is H_T. The electron-electron potentials are V_{01} and V_{02}. To solve this equation, we write $\left|\Psi\right\rangle$ as explicitly anti-symmetrized wave functions utilizing the multi-channel expansion

$$\Psi(x_0,x_1,x_2) = (1-P_{01}-P_{02})\sum_n \Phi_n(x_1,x_2) f_n(x_0), \tag{13}$$

where P_{01} and P_{02} are the space (coordinate and spin) exchange operator. The CC equations one gets upon inserting the eigenfunctions expansion are

$$\sum_n (K_0\delta_{mn} + V_{mn}) f_n = (E-\varepsilon_m) f_m, \tag{14}$$

where

$$V_{mn} = \left\langle \Phi_m \left| V \right| \Phi_n \right\rangle, \quad V = V_0 + V_{01} + V_{02} + (E-H)(P_{01}+P_{02}). \tag{15}$$

and $P_{0\alpha}$ are the space-exchange operator interchanging the coordinate labels for x_0 and $x_\alpha (\alpha = 1,2)$.

We define the coupled Lippmann-Schwinger equation for the *T*-matrix as

$$\left\langle \vec{k}_f^{(-)} \Phi_f \left| T \right| \Phi_i \vec{k}_i^{(+)} \right\rangle = \left\langle \vec{k}_f^{(-)} \Phi_f \left| V \right| \Phi_i \vec{k}_i^{(+)} \right\rangle +$$

$$+ \sum_n \int_k d^3k \frac{\left\langle \vec{k}_f^{(-)} \Phi_f \left| V \right| \Phi_n \vec{k} \right\rangle \left\langle \vec{k} \Phi_n \left| T \right| \Phi_i \vec{k}_i^{(+)} \right\rangle}{E^{(+)} - \varepsilon_n - k^2/2}, \tag{16}$$

where the projectile waves (discrete or continum) $\left| \vec{k} \right\rangle$ satisfy

$$\left(\varepsilon_k^{(\pm)} - K_0 \right) \left| \vec{k} \right\rangle = 0 \tag{17}$$

The on-shell momentum $\varepsilon_n = k_n^2/2$ are obtained from

$$E - \varepsilon_n - k_n^2/2 = 0, \tag{18}$$

and exist only for open channels *n* such that $E = \varepsilon_i - k_i^2/2 > \varepsilon_n$.

The partial wave Lippmann-Schwinger equation corresponding to Equation (16) for the reduced *T*-matrix elements are

$$\left\langle L_f k_f^{(-)}, f \pi_f l_f s_f \left\| T_{\Pi S}^{JN} \right\| L_i k_i^{(+)}, i \pi_i l_i s_i \right\rangle$$

$$= \left\langle L_f k_f^{(-)}, f \pi_f l_f s_f \left\| V_{\Pi S}^{JN} \right\| L_i k_i^{(+)}, i \pi_i l_i s_i \right\rangle$$

$$+ \sum_{n=1}^{N} \sum_{l,L} \int_k \frac{\left\langle L_f k_f^{(-)}, f \pi_f l_f s_f \left\| V_{\Pi S}^{JN} \right\| Lk^{(-)}, n \pi l s \right\rangle \left\langle Lk^{(-)}, n \pi l s \left\| T_{\Pi S}^{JN} \right\| L_i k_i^{(+)}, i \pi_i l_i s_i \right\rangle}{E - \varepsilon_n^N - k_n^2/2} dk. \tag{19}$$

The differential cross sections for scattering from channel i to channel f at an angle θ are given by

$$\frac{d\sigma_{fi}}{d\Omega} = (2\pi)^4 \frac{k_f}{k_i} \frac{\hat{S}^2}{\hat{l}^2} \sum_m \sum_{L_i, L_f, J} \left| \left\langle L_f k_f^{(-)}, n_f \pi_f l_f s_f \left| \left| T_{\Pi S}^{JN} \right| \right| L_i k_i^{(+)}, n_i \pi_i l_i s_i \right\rangle \right|^2. \quad (20)$$

The solution of Equations (19) and (20) are computed by Gaussian-type quadrature method.

TABLE 1: The configuration interaction coefficients and eigenvalues $(\varepsilon_{i_\alpha} + \varepsilon_{i_\beta})$ (a.u.), which are produced from non-orthogonal Laguerre-L^2 basis expansions, are shown for the ground states, $\lambda_{l_\alpha} = 4.0$ for $N_\alpha = 1$, $^{1,3}S$ excited states, $\lambda_{l_\beta} = 0.93$ for $N_\beta = 5,10,15$ and 20. Powers of ten are denoted by the number in brackets.

N_β	i_β	C_i^β (*singlet*)	^1S	C_i^β (*triplet*)	^3S
5	1	0.74808942	-2.145	0.87073610	-2.175
	2	0.14340948	-2.060	0.79678560(-1)	-2.068
	3	0.12524468	-2.027	0.46067410(-2)	-2.024
	4	0.20969070	-1.949	0.11558710(-1)	-2.022
	5	0.36419709	-1.430	0.88403520(-1)	-1.757
10	1	0.74803536	-2.145	0.88107540	-2.175
	2	0.14283304	-2.060	0.79419330(-1)	-2.068
	3	0.85402873(-1)	-2.033	0.38725260(-2)	-2.036
	4	0.71142478(-1)	-2.020	0.54271910(-2)	-2.022
	5	0.91485259(-1)	-2.003	0.55281310(-2)	-2.001
	6	0.11761430	-1.971	0.91031150(-2)	-1.956
	7	0.14979376	-1.908	0.16831390(-1)	-1.851
	8	0.19177824	-1.765	0.35179440(-1)	-1.521
	9	0.24834868	-1.333	0.85245700(-1)	-1.150
	10	0.32731445	1.234	0.22678300	0.622
15	1	0.74803535	-2.145	0.88109330	-2.175
	2	0.14283304	-2.060	0.79419330(-1)	-2.068
	3	0.85273406(-1)	-2.033	0.38725260(-2)	-2.036
	4	0.58862921(-1)	-2.021	0.51871930(-2)	-2.024
	5	0.52845917(-1)	-2.014	0.44492450(-2)	-2.015
	6	0.64270162(-1)	-2.005	0.42620740(-2)	-2.005
	7	0.76987035(-1)	-1.991	0.57706970(-2)	-1.989
	8	0.90433632(-1)	-1.970	0.80686310(-2)	-1.963

TABLE 1 (continued): The configuration interaction coefficients and eigenvalues $(\varepsilon_{i_\alpha} + \varepsilon_{i_\beta})$ (a.u.), which are produced from non-orthogonal Laguerre-L^2 basis expansions, are shown for the ground states, $\lambda_{l_\alpha} = 4.0$ for $N_\alpha = 1$, $^{1,3}S$ excited states, $\lambda_{l_\beta} = 0.93$ for $N_\beta = 5,10,15$ and 20. Powers of ten are denoted by the number in brackets.

N_β	i_β	C_i^β (***singlet***)	^1S	C_i^β (***triplet***)	^3S
	9	0.10556541	-1.938	0.11537710(-1)	-1.922
	10	0.12317497	-1.886	0.17145200(-1)	-1.850
	11	0.14409329	-1.799	0.26718840(-1)	-1.714
	12	0.16933340	-1.635	0.43916050(-1)	-1.405
	13	0.20029170	-1.272	0.76157350(-1)	-0.462
	14	0.23918206	-0.193	0.13722640	5.279
	15	0.28996389	6.027	0.24243530	7.258
20	1	0.74803535	-2.145	0.88109330	-2.175
	2	0.14283304	-2.060	0.79419330(-1)	-2.068
	3	0.85273406(-1)	-2.033	0.38725260(-2)	-2.036
	4	0.58631329(-1)	-2.021	0.51871930(-2)	-2.024
	5	0.44218265(-1)	-2.014	0.44367650(-2)	-2.016
	6	0.43505554(-1)	-2.010	0.35797390(-2)	-2.011
	7	0.51710191(-1)	-2.004	0.35903120(-2)	-2.004
	8	0.59818871(-1)	-1.995	0.45648320(-2)	-1.995
	9	0.67871562(-1)	-1.983	0.57940710(-2)	-1.982
	10	0.76336005(-1)	-1.967	0.73585380(-2)	-1.963
	11	0.85528142(-1)	-1.946	0.94600490(-2)	-1.937
	12	0.95714721(-1)	-1.916	0.12384490(-1)	-1.900
	13	0.10716038	-1.873	0.16572750(-1)	-1.845
	14	0.12015559	-1.809	0.22732620(-1)	-1.759
	15	0.13504246	-1.710	0.32026690(-1)	-1.612
	16	0.15225143	-1.543	0.46383180(-1)	-1.334
	17	0.17236660	-1.231	0.68955020(-1)	-0.713
	18	0.19625351	-0.543	0.10455180	1.156
	19	0.22532756	1.480	0.15905950	12.146
	20	0.26203222	12.975	0.23463870	13.250

TABLE 2: The configuration interaction coefficients and eigenvalues $(\varepsilon_{i_\alpha} + \varepsilon_{i\beta})$ (a.u.), which are produced from non-orthogonal Laguerre-L^2 expansions, are shown for the ground states, $\lambda_{l_\alpha} = 4.0$ for $N_\alpha = 1$, $^{1,3}P$ excited states, $\lambda_{l_\beta} = 0.72$ (*triplet*) and 0.73 (*singlet*) for $N_\beta = 5,10,15$ and 20. Powers of ten are denoted by the number in brackets.

N_β	i_β	C_i^β (***singlet***)	^1P	C_i^β (***triplet***)	^3P
5	1	0.52713383	-2.124	0.51845362	-2.133
	2	0.75194511(-1)	-2.055	0.47773401(-1)	-2.057
	3	0.70527762(-1)	-2.031	0.56809610(-1)	-2.031
	4	0.11918815	-2.000	0.98616618(-1)	-2.003
	5	0.22613564	-1.835	0.20712464	-1.847
10	1	0.52715943	-2.124	0.51776786	-2.133
	2	0.75194508(-1)	-2.055	0.47773401(-1)	-2.057
	3	0.63814190(-1)	-2.031	0.48819960(-1)	-2.032
	4	0.47330708(-1)	-2.020	0.39522669(-1)	-2.020
	5	0.52617990(-1)	-2.011	0.43224880(-1)	-2.012
	6	0.71621365(-1)	-1.996	0.60068528(-1)	-1.998
	7	0.95922494(-1)	-1.967	0.82810476(-1)	-1.970
	8	0.12631504	-1.903	0.11303319	-1.908
	9	0.15753703	-1.726	0.14688214	-1.738
	10	0.16452349	-0.925	0.15950565	-0.966
15	1	0.52715943	-2.124	0.51776787	-2.133
	2	0.75194508(-1)	-2.055	0.47773401(-1)	-2.057
	3	0.63814422(-1)	-2.031	0.48821071(-1)	-2.032
	4	0.46159286(-1)	-2.020	0.38807259(-1)	-2.020
	5	0.35793616(-1)	-2.014	0.30147522(-1)	-2.014
	6	0.37682827(-1)	-2.009	0.31154371(-1)	-2.009
	7	0.46860362(-1)	-2.002	0.39102629(-1)	-2.003
	8	0.56966251(-1)	-1.992	0.48192318(-1)	-1.993
	9	0.68449069(-1)	-1.975	0.58829337(-1)	-1.977
	10	0.81765562(-1)	-1.949	0.71581170(-1)	-1.952
	11	0.96911921(-1)	-1.906	0.86651429(-1)	-1.911
	12	0.11297434	-1.827	0.10340919	-1.835
	13	0.12707977	-1.662	0.11923534	-1.675
	14	0.13233640	-1.224	0.12719364	-1.253
	15	0.11417185	0.651	0.11198233	0.562

TABLE 2 (continued): The configuration interaction coefficients and eigenvalues $(\varepsilon_{i_\alpha} + \varepsilon_{i\beta})$ (a.u.), which are produced from non-orthogonal Laguerre-L^2 expansions, are shown for the ground states, $\lambda_{l_\alpha} = 4.0$ for $N_\alpha = 1$, $^{1,3}P$ excited states, $\lambda_{l_\beta} = 0.72$ (*triplet*) and 0.73 (*singlet*) for $N_\beta = 5,10,15$ and 20. Powers of ten are denoted by the number in brackets.

N_β	i_β	C_i^β (***singlet***)	^1P	C_i^β (***triplet***)	^3P
20	1	0.52715943	-2.124	0.51776787	-2.133
	2	0.75194508(-1)	-2.055	0.47773401(-1)	-2.057
	3	0.63814422(-1)	-2.031	0.48821072(-1)	-2.032
	4	0.46158409(-1)	-2.020	0.38807313(-1)	-2.020
	5	0.35032772(-1)	-2.014	0.29676385(-1)	-2.014
	6	0.28609943(-1)	-2.010	0.24139553(-1)	-2.010
	7	0.30630000(-1)	-2.007	0.25408294(-1)	-2.007
	8	0.36600637(-1)	-2.003	0.30557062(-1)	-2.003
	9	0.42651879(-1)	-1.996	0.35926131(-1)	-1.997
	10	0.49027727(-1)	-1.988	0.41692762(-1)	-1.989
	11	0.56006792(-1)	-1.976	0.48140072(-1)	-1.978
	12	0.63756102(-1)	-1.961	0.55464927(-1)	-1.963
	13	0.72348021(-1)	-1.938	0.63791996(-1)	-1.941
	14	0.81718667(-1)	-1.905	0.73131612(-1)	-1.909
	15	0.91567088(-1)	-1.854	0.83274234(-1)	-1.860
	16	0.10117139	-1.770	0.93590812(-1)	-1.779
	17	0.10907577	-1.619	0.10268428	-1.633
	18	0.11257588	-1.308	0.10781310	-1.332
	19	0.10690191	-0.499	0.10399619	-0.549
	20	0.83970711(-1)	2.888	0.82731961(-1)	2.734

ELASTIC SCATTERING

Elastic electron-helium scattering is well understood experimentally and theoretically and has been used extensively for calibration purposes in various electron-scattering applications. Therefore, we begin the presentation of differential cross sections by starting with intermediate energy elastic cross sections. The reported data set of elastic differential and integrated cross sections given by Register *et al*. (1980) at an impact energy range of 5-200 eV are in good agreement with the more recent study by Brunger *et al*. (1992) (1.5-50 eV).

Therefore, the results of the experiments of Register *et al*. (1980) (± 5 to 7% error bars) and Brunger *et al*. (1992) (± 3.5 to 5% error bars) are presented for comparison in this work. The calculations denoted by CCC and FOMBT are due to Fursa and Bray (1995) and Cartwright *et al*. (1992). The CCC and FOMBT cross sections are chosen because of established accuracy of this technique over a wide range of states and energies. The difference between the PC and CCC calculations are predominantly due to the inclusion of the different basis size in the CC formalism.

INELASTIC SCATTERING FROM THE GROUND STATE

In the Figures 4 to 15, we present the excitation differential cross sections of the 2^1S, 2^1P, 2^3S and 2^3P states calculated by the PSCC method for electron-helium scattering on the ground state at a range of projectile energies of 30, 40 and 50 eV. These are compared with the available experiments and theory. From the figures, we see that there is essentially complete qualitative, and often quantitative, agreement between the PC calculations and experiments of Trajmar *et al*. (1992) and Truhlar *et al*. (1973), Cartwright *et al*. (1992) and Khakoo *et al*. (1996) (± 10 to 20% error bars).

We note one exception to this at the forward and backward angles for the 2^1S, 2^1P, 2^3S and 2^3P excitations, where the PC values are considerably below the measurements of Trajmar *et al*. (1992) and Truhlar *et al*. (1973), Cartwright *et al*. (1992) and Khakoo *et al*. (1996). Discrepancies with the experiments and other theories are still substantial at the impact energy range of 30, 40 and 50 eV. The discrepancy between present work and experiments suggests that slightly large bases used in the calculations are necessary to get better accuracy.

INTEGRATED CROSS SECTIONS

Having presented differential cross sections, we now discuss the corresponding integrated cross sections. As the integrated cross sections are very important in practical applications, we give a more detailed convergence study here than for differential cross sections. It is important to note that we shall attempt to demonstrate convergence within the frozen-core approximation. We have no formal way of estimating the magnitude of the error of this approximation. Good agreement with angular dependent measurements suggests that generally this error will not often exceed 10%.

Upon examination of Table 3, we see generally good agreement with available measurements. Most encouraging is the excellent agreement at all energies with the measurements of integrated cross sections, where the errors are very small.

TABLE 3: Integrated cross sections (cm^2) for electrons scattering on the ground state of helium at 30, 40 and 50 eV. Square brackets denote powers of ten. The experimental measurements are due to Register *et al.*(1980) and Trajmar *et al.* (1992) (5% error). PC is due to present calculation and CCC to Fursa and Bray (1995).

State	Calculation and experiment	30 eV	40 eV	50 eV
1^1S	PC	2.23 [-16]	1.67 [-16]	1.28 [-16]
	CCC	2.25 [-16]	1.69 [-16]	1.34 [-16]
	Expt.	2.11 [-16]	1.58 [-16]	1.26 [-16]
2^3S	PC	1.91 [-18]	1.15 [-18]	7.51 [-16]
	CCC	1.91 [-18]	1.14 [-18]	7.32 [-16]
	Expt.	1.90 [-18]	1.18 [-18]	7.40 [-16]
2^1S	PC	2.30 [-18]	2.01 [-18]	1.74 [-18]
	CCC	2.19 [-18]	1.87 [-18]	1.67 [-18]
	Expt.	2.40 [-18]	2.11 [-18]	1.94 [-18]
2^3P	PC	2.58 [-18]	1.89 [-18]	1.30 [-18]
	CCC	2.19 [-18]	1.71 [-18]	1.07 [-18]
	Expt.	2.60 [-18]	1.90 [-18]	1.40 [-18]
2^1P	PC	3.80 [-18]	6.51 [-18]	8.16 [-18]
	CCC	3.86 [-18]	6.59 [-18]	8.18 [-18]
	Expt.	3.75 [-18]	6.43 [-18]	8.21 [-18]

CONCLUSIONS AND FUTURE WORK

Differential and integrated cross sections for electron scattering from a helium atom are calculated using an extension of a PSCC method developed for one electron target. Differential and integrated cross sections are found to be in good agreement with experimental measurements. Future plans will be to further extend the theory for the treatment of other open and closed shell atomic systems.

LIST OF FIGURES

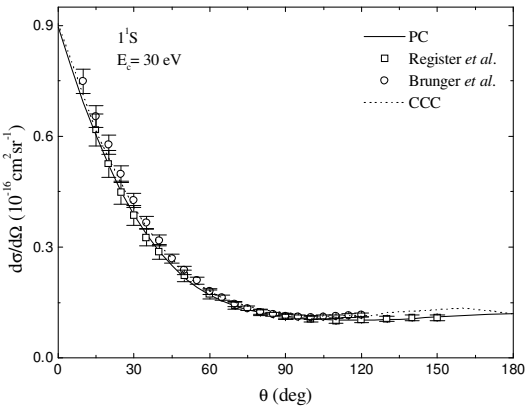

Figure 1: Elastic differential cross sections for electron-helium scattering at a projectile energy of 30 eV.

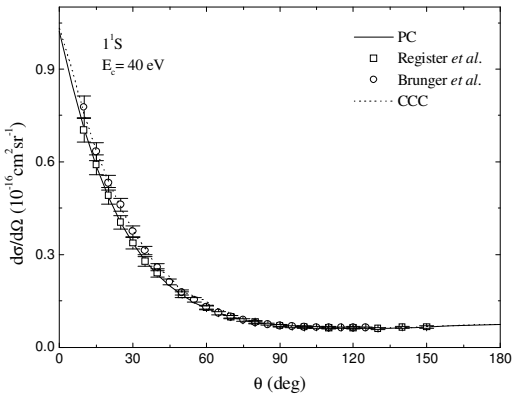

Figure 2: Elastic differential cross sections for electron-helium scattering at a projectile energy of 40 eV.

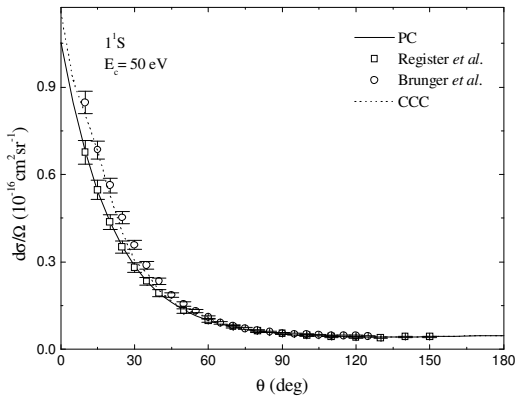

Figure 3: Elastic differential cross sections for electron-helium scattering at a projectile energy of 50 eV.

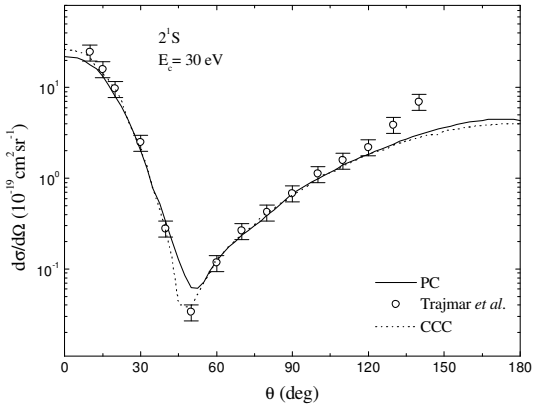

Figure 4: The 2^1S differential cross sections for electron-helium scattering at a projectile energy of 30 eV.

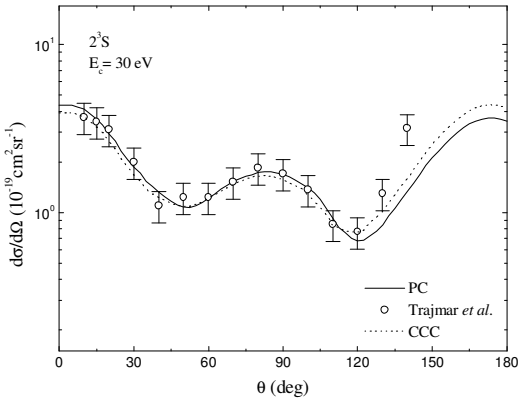

Figure 5: The 2^3S differential cross sections for electron-helium scattering at a projectile energy of 30 eV.

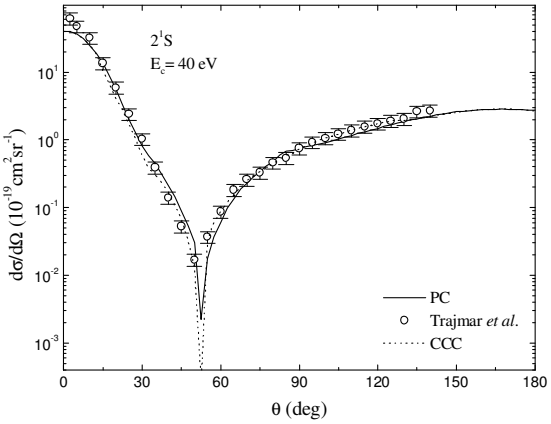

Figure 6: The 2^1S differential cross sections for electron-helium scattering at a projectile energy of 40 eV.

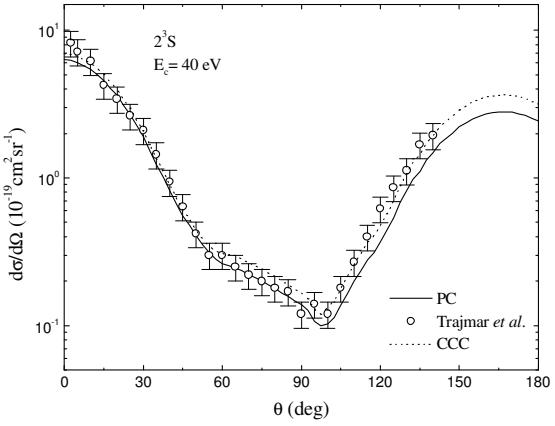

Figure 7: The 2^3S differential cross sections for electron-helium scattering at a projectile energy of 40 eV.

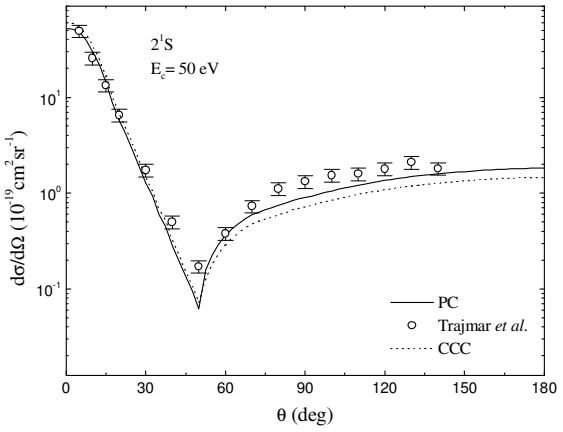

Figure 8: The 2^1S differential cross sections for electron-helium scattering at a projectile energy of 50 eV.

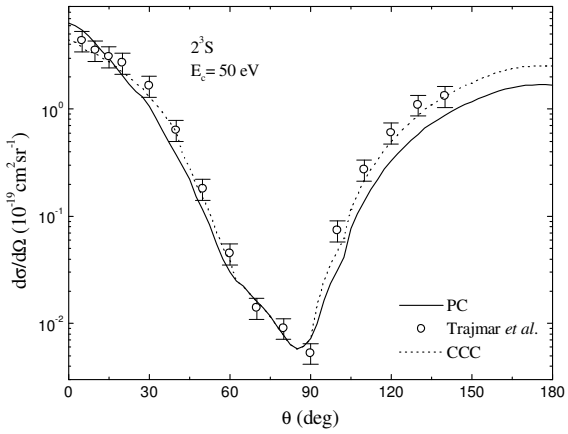

Figure 9: The 2^3S differential cross sections for electron-helium scattering at a projectile energy of 50 eV.

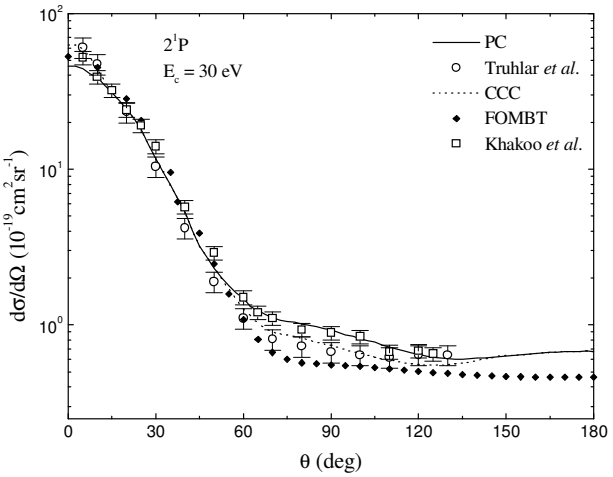

Figure 10: The 2^1P DCS for electron-helium scattering at a projectile energy of 30 eV.

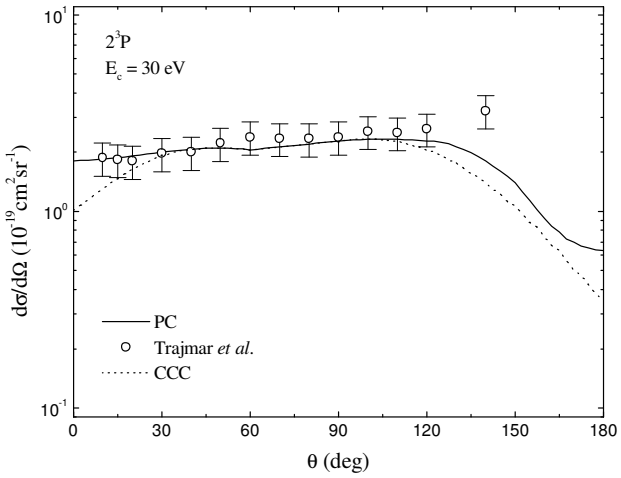

Figure 11: The 2^3P differential cross sections for electron-helium scattering at a projectile energy of 30 eV.

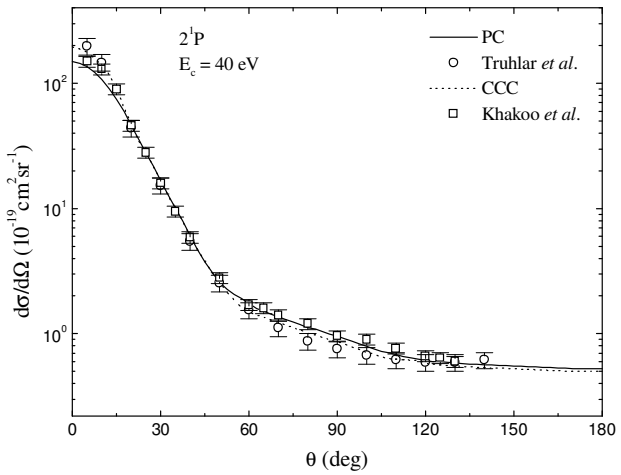

Figure 12: The 2^1P DCS for electron-helium scattering at a projectile energy of 40 eV.

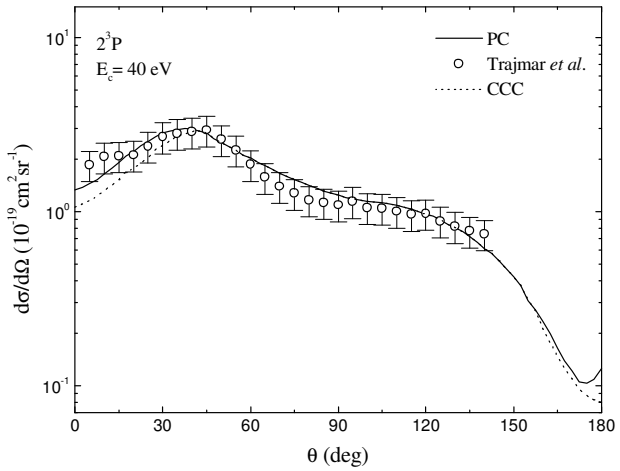

Figure 13: The 2^3P differential cross sections for electron-helium scattering at a projectile energy of 40 eV.

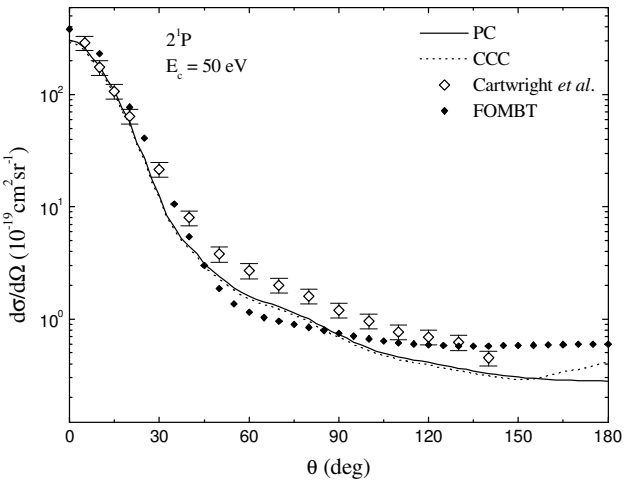

Figure 14: The 2^1P DCS for electron-helium scattering at a projectile energy of 50 eV.

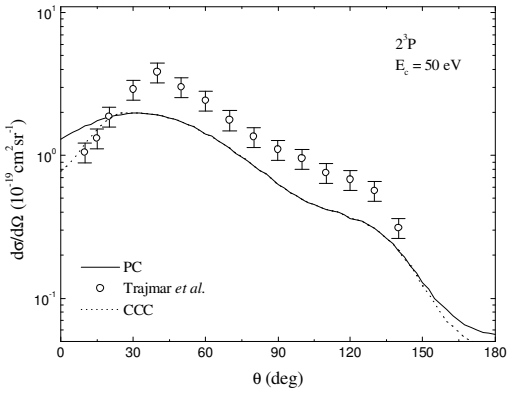

Figure 15: The 2^3P differential cross sections for electron-helium scattering at a projectile energy of 50 eV.

ACKNOWLEDGEMENTS

The authors like to thank Prof. Andris Stelbovics and Prof. Igor Bray for their helpful references they supplied.

REFERENCES

Bartschat, K., Hudson, E. T., Scott, M. P., Burke, P. G. and Burke,V. M. 1996. Differential cross sections and electron-impact coherence parameters for electron scattering from helium atoms, *J. Phys. B: At. Mol. Opt. Phys.,* **29**: 2875-2886.

Bray, I. and Stelbovics, A. T. 1992. Convergent close-coupling calculations of electron-hydrogen scattering, *Phys. Rev. A,* **46**: 6995-7011.

Brunger, M. J., Buckman, S. J., Allen, L. J., McCarthy, I. E. and Ratnavelu, K. 1992. Elastic electron scattering from helium: absolute experimental cross section, theory and derived potentials, *J. Phys. B: At. Mol. Opt. Phys.,* **25**: 1823-1838.

Cartwright, D. C., Csanak, G., Trajmar, S. and Register, D. F. 1992. Electron-impact excitation of the n^1P levels of helium: Theory and experiment, *Phys. Rev. A,* **45**:1602-1624.

Fursa, D. V. and Bray, I. 1995. Calculation of electron-helium scattering, *Phys. Rev. A*, **52**: 1279-1297.

Kartono, A., Winata, T. and Sukirno. 2005. Applications of non-orthogonal Laguerre function basis in helium atom, *Appl. Math. Comp.,* **163**: 879–893.

Khakoo, M. A., Roundy, D. and Rugamas, F. 1996. Electron-impact excitation of the $1^1S \rightarrow 3^1P$ and $1^1S \rightarrow 4^1P$ transitions in helium, *Phys. Rev. A,* **54**: 4004-4014.

Register, D. F., Trajmar, S. and Srivastava, S. K. 1980. Absolute elastic differential electron scattering cross section for He: a proposed calibration standard from 5 to 200 eV, *Phys. Rev. A*, **21**:1134-1151.

Trajmar, S., Register, D. F., Cartwright, D.C. and Csanak, G. 1992. Differential and integral cross section for electron impact excitation of the n^3S, n^1S and n^3P (n = 2, 3) levels in He, *J. Phys. B: At. Mol. Opt. Phys.,* **25**: 4889-4910.

Truhlar, D. G., Trajmar, S., Williams, W., Ormonde, S. and Torres, B. 1973. Quantum-mechanical and experimental study of the excitation of the 2^1P state of He by electron impact at 29-40 eV, *Phys. Rev. A,* **8**: 2475-2482.

Winata, T. and Kartono, A. 2004. Study of non-orthogonal Laguerre-L^2 method for helium atom, *Eur. Phys. J. D: At. Mol. Opt. Phys*., **28**: 307-315.